Universality in chaotic quantum transport: The concordance between random matrix and semiclassical theories

Gregory Berkolaiko[1] and Jack Kuipers[2]

[1] *Department of Mathematics, Texas A&M University, College Station, TX 77843-3368, USA*
[2] *Institut für Theoretische Physik, Universität Regensburg, D-93040 Regensburg, Germany*

(Dated: May 29, 2018)

Electronic transport through chaotic quantum dots exhibits universal, system independent, properties, consistent with random matrix theory. The quantum transport can also be rooted, via the semiclassical approximation, in sums over the classical scattering trajectories. Correlations between such trajectories can be organized diagrammatically and have been shown to yield universal answers for some observables. Here, we develop the general combinatorial treatment of the semiclassical diagrams, through a connection to factorizations of permutations. We show agreement between the semiclassical and random matrix approaches to the moments of the transmission eigenvalues. The result is valid for all moments to all orders of the expansion in inverse channel number for all three main symmetry classes (with and without time reversal symmetry and spin-orbit interaction) and extends to nonlinear statistics. This finally explains the applicability of random matrix theory to chaotic quantum transport in terms of the underlying dynamics as well as providing semiclassical access to the probability density of the transmission eigenvalues.

PACS numbers: 05.45.Mt, 73.23.-b, 03.65.Nk, 03.65.Sq

Closed mesoscopic systems with sizes between the atomic and macroscopic possess statistically different energy spectra depending on whether the corresponding classical system is regular or chaotic [1, 2]. A semiclassical approach to such systems, valid in the effective limit of $\hbar \to 0$, leads to trace formulae where the density of energy states is approximated by sums over the classical periodic orbits of the system [3, 4] which form stable families for regular systems while being unstable and isolated in chaotic ones. A hallmark of the energy statistics is the form factor, a two-point correlation function approximated by a double sum over periodic orbits. By pairing orbits with themselves for chaotic systems or members of their families for regular ones, the difference between their corresponding energy spectra can be directly linked to the properties of the underlying dynamics [5, 6].

For (quantum) chaotic systems, there is the further conjecture [7] that the statistics of the energy spectra are universal (depending just on the symmetry of the system) and identical to those of the eigenvalues of large random matrices [8], originally employed to model the spectra of atomic nuclei. However, the semiclassical pairing of periodic orbits with themselves [6] only led to agreement with the leading order term of the random matrix theory (RMT) form factor. Recently, additional correlated periodic orbits were identified, treated and shown to provide exact agreement with RMT for short times [9, 10]. This involves orbits which come close to themselves in an 'encounter', whose occurrence can be estimated using the ergodicity of the classical motion, and partner orbits which can be constructed, due to the local hyperbolicity, to cross the encounter differently. For long times the correlations remain unknown, but the form factor can be obtained through resummation of short orbits [11–13].

Hallmarks of the underlying dynamics persist in open systems, obtained by attaching scattering leads, as seen for example in an experimental study of the electronic transport through quantum dots [14]. Theoretically, we start with the transmission subblock t of the scattering matrix connecting asymptotic states in the (two) leads. The transmission eigenvalues of the matrix $T = t^\dagger t$, and their moments $M_n = \mathrm{Tr}[T^n]$ relate to the electronic flow through the system. For example in the low temperature limit the first moment is proportional to the conductance [15, 16].

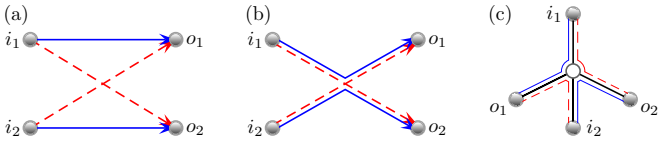

FIG. 1. (Color online) (a) The trajectories for M_2 form a closed cycle if the dashed trajectories, which contribute with negative action, are traversed backwards. (b) To contribute in the semiclassical limit, the trajectories must be nearly identical apart from in small encounter regions which they can traverse differently. (c) By untwisting the encounter, the diagram in (b) can be redrawn as the boundary walk of a tree.

For ballistic chaotic systems, modeling the scattering matrix by a random matrix from the circular ensembles was proposed and shown to be consistent with a diagonal semiclassical approach [17]. For the low moments M_1 and M_2, all off-diagonal contributions were evaluated in [18–20], while the calculation of general M_n, but only for the first several off-diagonal terms, were performed in [21, 22]. In all cases, the results agree with RMT. The purpose of this letter is to exhibit the mathematical reasons behind this agreement and establish the general equivalence between semiclassics for open systems and RMT of the circular ensembles. The derivation extends

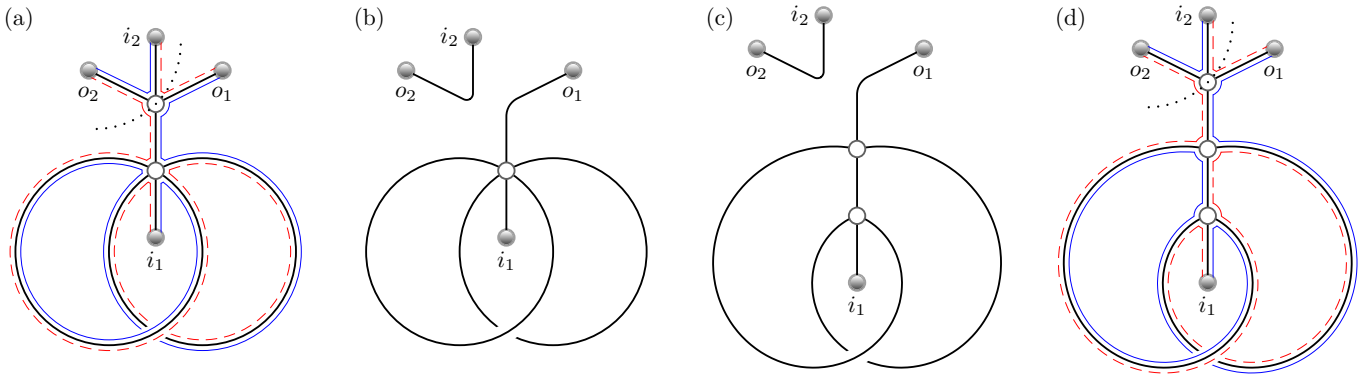

FIG. 2. (Color online) The graph in (a) and its boundary walk represent a trajectory quartet which would contribute to M_2. Following steps 1–5 we first cut the top encounter node (keeping o_2 connected to i_2) and arrive at (b). As o_1 is now attached to a node of degree 6 we insert a new link to obtain (c). Reconnecting the link from i_2 to o_2 we obtain a second trajectory quartet in (d) which exactly cancels the contribution from (a). Performing steps 1–5 on (d) reverses the chain to recover (a).

to all three main symmetry classes: unitary for chaotic systems without time reversal symmetry (TRS), orthogonal for systems with TRS and symplectic for systems with spin-orbit interaction. It also remains valid for the nonlinear moments.

Our approach holds in the universal regime where the dwell time, the average time spent inside the system, is much longer than the Ehrenfest time $\tau_{\rm E}$, the time needed for a wavepacket of size $\lambda_{\rm F}$, the Fermi wavelength, to grow to the system size L and delocalize. Under chaotic dynamics, with Lypunov exponent λ, we have $\tau_{\rm E} \approx \lambda^{-1} \ln(L/\lambda_{\rm F})$ and when no longer small compared to the dwell time, RMT stops being applicable. However, such Ehrenfest time effects have been incorporated into the semiclassical framework for all diagrams at leading order and some subleading order diagrams for low moments [23–26]. Our systematic approach may then be useful beyond the universal regime.

RMT results. RMT provides the joint probability distribution of the transmission eigenvalues [27] which can be integrated to obtain the transport moments, as was performed for the conductance and its variance [28, 29]. Other quantities were limited to diagrammatic expansions [30] until the connection to the Selberg integral was explored [31, 32]. Since then there has been much interest and success in calculating the moments M_n from the circular ensembles [33–36].

Semiclassical diagrams. Semiclassically, the elements t_{oi} of the scattering matrix are approximated [18, 37, 38] by a sum over the trajectories γ which start in channel i in one lead and end in channel o of the other. They contribute a phase $\exp(\mathrm{i}S_\gamma/\hbar)$ with their action S_γ so that M_n is approximated by a sum over $2n$ trajectories of which half contribute with positive action and travel from channels i_j to o_j while the other half contribute with negative action and travel from channels i_{j+1} to o_j (we identify i_{n+1} with i_1). Geometrically, if we reverse the direction of the trajectories with negative action, the trajectories would form a single cycle visiting $i_1, o_1, i_2, \ldots$ in turn, as in Fig. 1(a). The phase involving the actions oscillates in the semiclassical limit unless the total action difference is small on the scale of $\hbar$. To obtain the statistical properties of the moments we average over a range of energies so that oscillating phases wash out and only trajectory sets which achieve this small action difference contribute consistently. These, as for closed systems, come close in encounters while being nearly identical elsewhere (in 'links'), as in Fig. 1(b).

For M_1 (conductance), we have trajectory pairs starting and ending together, and the contributing semiclassical diagrams were identified and treated [19] precisely by cutting open the periodic orbit diagrams of the form factor. For M_2, which is related to the shot noise, the contributing trajectory quadruplets can be formed by cutting periodic orbits twice [20], and this approach has been generalised in the complementary work of Ref. [39].

The contribution of each semiclassical diagram is a simple product of its constituent parts [20]. If the leads carry N_1 and N_2 channels respectively (with a total $N = N_1 + N_2$) then each incoming channel provides the factor N_1 and each outgoing channel N_2. More importantly, each link provides a factor of $1/N$ and each encounter $-N$. Assuming $N_1 \sim N_2$, the order in N^{-1} of each diagram is the difference between the number of links and the number of encounters (and channels). The leading order diagrams can then be redrawn as trees, or rather as paths around the tree along the so-called 'boundary walk' [21]. The encounters are untwisted to become roundabout nodes, the links edges and the channels leaves, so Fig. 1(b) morphs to Fig. 1(c). The leading order of all M_n was obtained in [21] by recursively generating the trees. Higher order diagrams involve closed cycles and a graphical representation provided moment generating functions at the next two orders [22] which match an asymptotic expansion of RMT results [36]. We now build on this to show exact concordance between

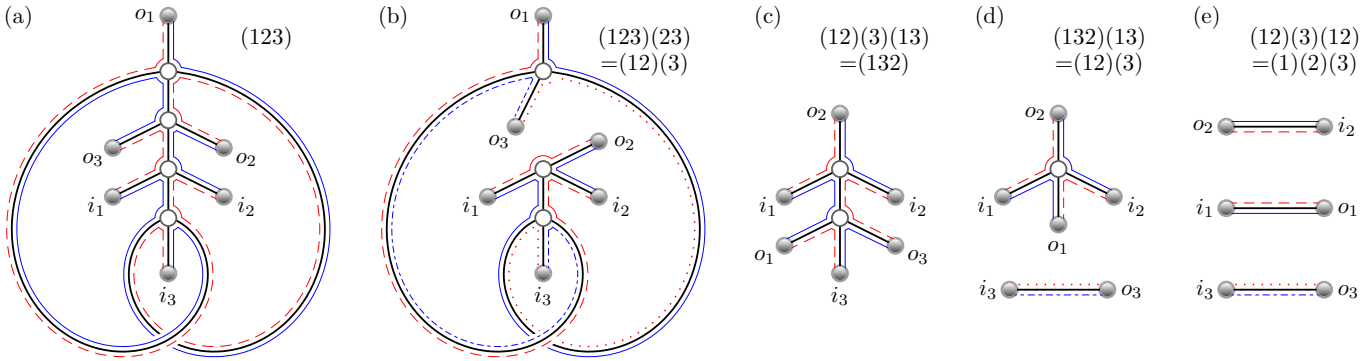

FIG. 3. (Color online) The trajectory sextet in (a) form a single cycle or the permutation (123). Untying the node with leaves o_3 and o_2 (keeping o_3 connected to i_3) breaks the single cycle into two and corresponds to multiplying (123) by (23) to obtain (12)(3) as in (b). Repeating the untying we move through (c) and (d) until we reach separated links in (e) or the identity permutation. Inverting the steps we can represent the original diagram in (a) as the primitive factorization (12)(13)(13)(23)=(123).

semiclassics and RMT for all moments and to all orders.

Cancellations. First we show that the vast majority of possible semiclassical diagrams cancel. Since each encounter leads to a minus factor, we will pair up diagrams that differ by one encounter and one link to mutually cancel before counting the surviving diagrams. The pairing is realized using the following recursive procedure:

1. Find the outgoing leaf o_m (attached to an encounter node) with maximal m.
2. If o_m is attached to a node of degree 4 whose opposite edge ends in a leaf, untie the node.

To untie a node we break it into two parts keeping the path connecting i_m to o_m intact. This may separate a link directly connecting i_m to o_m from the rest of the diagram. Such a link is removed from further consideration. We repeat steps 1 and 2 while it remains possible. For example, from Fig. 2(a) we separate the top encounter into two parts to give us Fig. 2(b) and reduce m to 1.

Once we can no longer perform step 2, we perform either of the following steps:

3. If o_m is attached to a node of degree 4 whose opposite edge ends in another encounter node, shrink the edge and join the two nodes together.
4. Otherwise, separate o_m and its two neighbors from the encounter by inserting a new link.

These two operations are inverses of each other and provide the required difference in the number of encounters [see Figs. 2(b) and (c)]. Finally we:

5. reverse all the operations performed at step 2.

We thus reconstruct a diagram paired to the original one, with a contribution of opposite sign. All diagrams that ever arrive at step 3 or 4 cancel with their partner, as, for example, the diagrams in Figs. 2(a) and (d).

Factorizations of permutations. Diagrams that never reach step 3 or 4 can only involve encounter nodes of degree 4 and, following steps 1 and 2 repeatedly, must eventually end up as a set of independent links connecting each i_j to its o_j. For M_n we initially have trajectories along the boundary walk visiting the channels $i_1 \to o_1 \to i_2 \ldots o_n \to i_1$ which we can represent as the cyclic permutation $\sigma_n = (12\ldots n)$. For systems without time reversal symmetry, when we arrive at step 2 for the first time we must have some o_j opposite o_n. The operation of untying is equivalent to multiplying σ_n by the transposition $(j\,n)$, breaking the boundary walk into two cycles, $\sigma_n(j\,n) = (1\ldots j)(j+1\ldots n)$. Repeating steps 1 and 2 we multiply repeatedly on the right by the pair of o channel labels at each step 2 until we arrive at the independent links whose boundary walk is the identity permutation. Reversing the untying of the nodes, we obtain a factorization of σ_n in terms of transpositions, which represents the original diagram. This process is illustrated in Fig. 3. Because we always chose the o_m with the maximal m at each step 1, the resulting factorization $(s_1\,t_1)\ldots(s_d\,t_d)$ can be written so that $t_j > s_j$ and $t_k \geq t_j$ for all $k \geq j$. Such a factorization is called 'primitive' and its depth d is the number of nodes untied at step 2, each of which removes two links and one encounter. The number of encounters in the diagram is equal to d and the number of links $n+2d$. Diagrams without time reversal symmetry that survive the cancellation are therefore labeled by primitive factorizations and provide the semiclassical contribution $(-1)^d N_1^n N_2^n / N^{n+d}$.

Encounters in the lead. One complication is encounters that occur in the leads. For example, we could push the encounter in Fig. 1(b) to the left into the lead so that the incoming channels coincide $i_1 = i_2$. We then lose two links, the encounter itself and one channel so that the new diagram still contributes at the same order but as $N_1 N_2^2/N^3$ instead of $-N_1^2 N_2^2/N^4$. Likewise we could move the encounter to the right until the outgoing channels coincide and the full contribution of diagrams related to Fig. 1(b) is the sum of these three possibilities.

Whether encounters can be placed in the lead can be

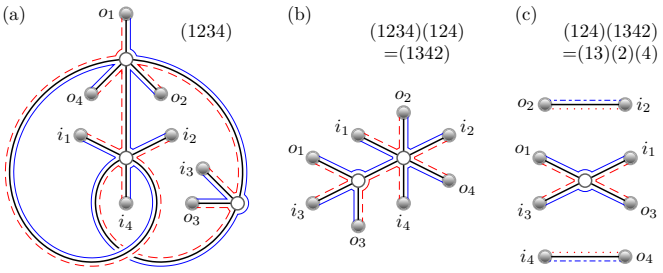

FIG. 4. (Color online) The top node in (a) may move into the outgoing lead which, by untying, we can represent as the permutation (1234)(124)=(1342) and the boundary walk in (b). Also placing the central node in (a) in the incoming lead means we further multiply on the left by (124) to obtain (c).

seen directly from the graphical representation. If every alternate link of a node ends in an i leaf, then the encounter can be placed in the incoming lead and similarly for the outgoing lead. Once encounters are in the leads, they can no longer be joined or separated as in steps 3 and 4. Instead, we consider the encounters in the leads as being already untied. Then we perform the procedure above to identify canceling pairs. Each node in the outgoing lead corresponds to multiplying σ_n on the right by the cycle of the labels of the o leaves (read off clockwise). Nodes placed in the incoming lead multiply the permutation on the left by the cycle of their i labels, illustrated in Fig. 4. For the resulting permutation all non-canceling diagrams are again labeled by the primitive factorizations of the permutation in question.

Equivalence with RMT. The semiclassical result is

$$M_n = \sum_{\chi_i,\chi_o} \frac{N_1^{c(\chi_i)} N_2^{c(\chi_o)}}{N^n} \sum_d \frac{(-1)^d p_d(\chi_i \sigma_n \chi_o)}{N^d} \qquad (1)$$

where $p_d(\cdot)$ is the number of primitive factorizations of depth d, and $c(\cdot)$ the number of cycles. In the sum over all possible permutations χ_i and χ_o, their cycles represent incoming and outgoing channels which coincide. For example, the diagram in Fig. 4(a) contributes to the fourth moment when the top and central nodes are placed in the leads, $\chi_i = \chi_o = (124)(3)$. The resulting primitive factorization (13) leads to the contribution $-N_1^2 N_2^2/N^5$. For M_2, the only primitive factorizations are $(12)^d$ with odd and even d being factorizations of (12) and (1)(2) respectively, which are also the two possibilities for χ_i and χ_o. This gives $M_2 = N_1 N_2/N - N_1^2 N_2^2/(N^3 - N)$.

The random matrix result, on the other hand, can be written exactly as in Eq. (1) but replacing $\sum_d (-1)^d p_d(\pi)/N^{n+d}$ by coefficients $V(\pi)$; see [30, 40, 41]. That $V(\pi)$ is the generating function for the number of primitive factorizations $p_d(\pi)$ was recently established [42] using an expression for $V(\pi)$ in terms of characters of the symmetric group. Here we sketch a simple alternative proof that is easy to generalize to systems with TRS. The $p_d(\pi)$ only depend on the cycle structure of π so let $c_1, \ldots, c_k$ be the lengths of the cycles in the permutation $\pi = (12\ldots c_k)\cdots(n - c_1 + 1 \ldots n)$. First consider the case when the term on the right of a primitive factorization of π is of the form $(s_d\, n)$. Without this term, it is a factorization (of depth $d-1$) of the permutation $\pi(s_d\, n)$. If s_d belongs to the rightmost cycle of π it splits into two, of lengths q and r with $q + r = c_1$, while if s_d belongs to cycle j the rightmost cycle joins with it to form a cycle of length $c_1 + c_j$. Finally, the last term $(s_d\, t_d)$ can have $t_d \neq n$ only if $c_1 = 1$ and the factorization does not have any occurrence of n in it. In this case it is also a factorization of the permutation on $n-1$ elements with cycle lengths $c_2, \ldots, c_k$. In total we have

$$p_d(c_1, \ldots, c_k) = \delta_{c_1,1} p_d(c_2, \ldots, c_k) + \sum_{c_j} c_j p_{d-1}(c_1 + c_j, \ldots) + \sum_{q,r=c_1} p_{d-1}(q, r, c_2, \ldots, c_k)$$

exactly mirroring the recursion relations of V [40].

Time reversal symmetry. With TRS the semiclassical diagrams are more complicated [22], and the relevant combinatorial objects are permutations on $2n$ elements $\bar{n}, \ldots, \bar{1}, 1, \ldots, n$. The starting permutation with no encounters in leads is encoded by $\tilde{\sigma}_n = (\bar{n}\ldots\bar{1})(1\ldots n)$. The cancellation procedure remains the same, but now it is also possible to untie nodes which have an i_j leaf opposite o_m, which we represent by multiplication on the right by $(\bar{j}\, m)$ and on the left by $(\bar{m}\, j)$ [untying o_j and o_m also multiplies by $(\bar{m}\, \bar{j})$ on the left in addition to $(j\, m)$ on the right]. The non-canceling factorizations are then of the form $\tilde{p}_d(\tilde{\sigma}_n) = (\bar{t}_d\, \bar{s}_d)\cdots(\bar{t}_1\, \bar{s}_1)(s_1\, t_1)\cdots(s_d\, t_d)$ with $t_j > s_j$ and $t_k \geq t_j, \bar{t}_j, \bar{s}_j$ for all $k \geq j$.

Since the two leads for the transmission are separate, still only nodes with alternating i or o leaves can move into the leads and we obtain a result like Eq. (1) but involving the doubled permutations. Following similar reasoning to above, the $\tilde{p}_d(\tilde{\pi})$ satisfy the same recursion relations as the coefficients V from the circular orthogonal ensemble so the moments are identical.

Spin-orbit interaction. The semiclassical framework includes spin-orbit interaction through an additional trace of a product of spin propagators along the trajectories [43]. The structure of the leading order diagrams makes this product identity and effectively leaves the leading order of M_n unchanged [44]. For each order higher in inverse channel number, the chaotic spin-orbit interaction provides an additional factor of $-1/2$ (for spin $1/2$) compared to the contributions with TRS [44]. The cancellation procedure then still holds, and the effect can be included by simply substituting $N_1 \to -2N_1$, $N_2 \to -2N_2$ and multiplying by $-1/2$. This is the same mapping as between the orthogonal and symplectic RMT ensembles [30] so the moments are again identical.

Conclusions. Though we focused on the moments of the transmission eigenvalues, the combinatorial treatment here extends to non-linear statistics by simply changing the starting permutation σ_n. Moreover, since

we have an exact concordance between the semiclassical and RMT [33–36] moments of the transmission eigenvalues, we obtain their probability distribution semiclassically. Indirectly, any RMT result derived from this distribution, for example the nonlinear statistics in [32] and the moments of the conductance and shot noise [34, 45, 46], is now rooted in the chaotic dynamics inside the cavity and the correlations between scattering trajectories.

For energy dependent correlation functions, diagrams related to each other by the cancellation procedure no longer cancel exactly. For the related quantities of Andreev billiards and Wigner delay times, the agreement between semiclassics and RMT remains limited to leading [47, 48] and several subleading orders [22, 36, 49] respectively.

Finally, with the close connection between ballistic chaotic systems, RMT and systems with weak disorder, the combinatorial ideas here should have parallels in the diagrammatic perturbation theory of disorder. They also form the start point of including Ehrenfest time effects [23–26] beyond the RMT regime.

Acknowledgments. We would like to thank Juan Diego Urbina and Klaus Richter for helpful comments and discussion as well as Marcel Novaes for sharing his alternative method and results [39]. GB is funded by NSF award DMS-0907968 while JK acknowledges funding from the DFG through research unit FOR760.

[1] M. C. Gutzwiller, *Chaos in classical and quantum mechanics* (Springer, New York, 1990).
[2] F. Haake, *Quantum signatures of chaos*, 3rd ed. (Springer, Berlin, 2010).
[3] M. C. Gutzwiller, J. Math. Phys. **12**, 343 (1971).
[4] R. Balian and C. Bloch, Ann. Phys. **85**, 514 (1974).
[5] J. H. Hannay and A. M. Ozorio de Almeida, J. Phys. A **17**, 3429 (1984).
[6] M. V. Berry, Proc. Roy. Soc. A **400**, 229 (1985).
[7] O. Bohigas, M. Giannoni, and C. Schmit, Phys. Rev. Lett. **52**, 1 (1984).
[8] M. L. Mehta, *Random matrices*, 3rd ed. (Elsevier, Amsterdam, 2004).
[9] M. Sieber and K. Richter, Phys. Scr. **T90**, 128 (2001).
[10] S. Müller, S. Heusler, P. Braun, F. Haake, and A. Altland, Phys. Rev. Lett. **93**, 014103 (2004); Phys. Rev. E **72**, 046207 (2005).
[11] S. Heusler, S. Müller, A. Altland, P. Braun, and F. Haake, Phys. Rev. Lett. **98**, 044103 (2007).
[12] J. P. Keating and S. Müller, Proc. Roy. Soc. A **463**, 3241 (2007).
[13] S. Müller, S. Heusler, A. Altland, P. Braun, and F. Haake, New J. Phys. **11**, 103025 (2009).
[14] A. M. Chang, H. U. Baranger, L. N. Pfeiffer, and K. W. West, Phys. Rev. Lett. **73**, 2111 (1994).
[15] R. Landauer, IBM J. Res. Dev. **1**, 223 (1957); **33**, 306 (1988).
[16] M. Büttiker, Phys. Rev. Lett. **57**, 1761 (1986).
[17] R. Blümel and U. Smilansky, Phys. Rev. Lett. **60**, 477 (1988); **64**, 241 (1990).
[18] K. Richter and M. Sieber, Phys. Rev. Lett. **89**, 206801 (2002).
[19] S. Heusler, S. Müller, P. Braun, and F. Haake, Phys. Rev. Lett. **96**, 066804 (2006).
[20] S. Müller, S. Heusler, P. Braun, and F. Haake, New J. Phys. **9**, 12 (2007).
[21] G. Berkolaiko, J. M. Harrison, and M. Novaes, J. Phys. A **41**, 365102 (2008).
[22] G. Berkolaiko and J. Kuipers, New J. Phys **13**, 063020 (2011).
[23] R. S. Whitney and Ph. Jacquod, Phys. Rev. Lett. **96**, 206804 (2006); Ph. Jacquod and R. S. Whitney, Phys. Rev. B **73**, 195115 (2006).
[24] P. W. Brouwer and S. Rahav, Phys. Rev. B **74**, 075322 (2006); **74**, 085313 (2006).
[25] D. Waltner and J. Kuipers, Phys. Rev. E **82**, 066205 (2010).
[26] D. Waltner, J. Kuipers, and K. Richter, Phys. Rev. B **83**, 195315 (2011).
[27] C. W. J. Beenakker, Rev. Mod. Phys. **69**, 731 (1997).
[28] H. U. Baranger and P. A. Mello, Phys. Rev. Lett. **73**, 142 (1994).
[29] R. A. Jalabert, J. Pichard, and C. W. J. Beenakker, Europhys. Lett. **27**, 255 (1994).
[30] P. W. Brouwer and C. W. J. Beenakker, J. Math. Phys. **37**, 4904 (1996).
[31] D. V. Savin and H. Sommers, Phys. Rev. B **73**, 081307 (2006).
[32] D. V. Savin, H. Sommers, and W. Wieczorek, Phys. Rev. B **77**, 125332 (2008).
[33] P. Vivo and E. Vivo, J. Phys. A **41**, 122004 (2008).
[34] M. Novaes, Phys. Rev. B **78**, 035337 (2008).
[35] G. Livan and P. Vivo, Acta Phys. Pol. B **42**, 1081 (2011).
[36] F. Mezzadri and N. Simm, J. Math. Phys. **52**, 103511 (2011); arXiv:1108.2859.
[37] W. H. Miller, Adv. Chem. Phys. **30**, 77 (1975).
[38] K. Richter, *Semiclassical theory of mesoscopic quantum systems* (Springer, Berlin, 2000).
[39] M. Novaes, arXiv:1111.5179.
[40] S. Samuel, J. Math. Phys. **21**, 2695 (1980).
[41] P. A. Mello, J. Phys. A **23**, 4061 (1990).
[42] S. Matsumoto and J. Novak, Discrete Math. Theor. Comput. Sci. (FPSAC 2010), 403 (2010).
[43] O. Zaitsev, D. Frustaglia, and K. Richter, Phys. Rev. Lett. **94**, 026809 (2005); Phys. Rev. B **72**, 155325 (2005).
[44] D. Waltner and J. Bolte, Phys. Rev. B **76**, 075330 (2007); D. Waltner, private communication.
[45] V. A. Osipov and E. Kanzieper, Phys. Rev. Lett. **101**, 176804 (2008); J. Phys. A **42**, 475101 (2009).
[46] B. A. Khoruzhenko, D. V. Savin, and H. Sommers, Phys. Rev. B **80**, 125301 (2009).
[47] J. Kuipers, D. Waltner, C. Petitjean, G. Berkolaiko, and K. Richter, Phys. Rev. Lett. **104**, 027001 (2010); J. Kuipers, T. Engl, G. Berkolaiko, C. Petitjean, D. Waltner, and K. Richter, Phys. Rev. B **83**, 195316 (2011).
[48] J. A. Melsen, P. W. Brouwer, K. M. Frahm, and C. W. J. Beenakker, Europhys. Lett. **35**, 7 (1996); Phys. Scr. **T69**, 223 (1997).
[49] G. Berkolaiko and J. Kuipers, J. Phys. A **43**, 035101 (2010).